scientific reports

Check for updates

OPEN

Safety risk assessment of reservoir dam structure: an empirical study in China

Dingying Yang[1], Jiamei Wu[1], Zhenxu Guo[2]✉, Xiaoye Zeng[3]✉ & Qianqian Zhang[1]

Reservoir dam structure is critical to protect public life and property and has always been attention worldwide. However, a systematic approach to assessing the safety risks of reservoir dam structure (RDS) is still required. This study presents a holistic framework for evaluating the safety risk of RDS and develops an evaluation index system. A risk assessment model is constructed based on the cloud and Dempster-Shafer (D-S) evidence theories. The model's validity is confirmed through an empirical analysis of the XY reservoir project. This study offers theoretical insights and practical solutions for managers to facilitate decision-making and supports the advancement of industry standards.

Keywords Reservoir dam structure, Safety risk, Assessment, Cloud model, D-S evidence theory

Fighting with nature in exchange for a comfortable and secure living environment has been the constant pursuit of human beings for thousands of years. The erection of reservoir dams is a significant event in the transformation of nature by man, nevertheless, we have not tamed nature. Over the past few decades, safety accidents have become a global concern, including reservoir overflow, dam landslides, and dam collapse[1–3].

In the mid-twentieth century, dam breaks occurred frequently, resulting immeasurable loss. According to China's dam database, there were 3358 dam accidents from 1954 to 2021[4]. Between 1954 and 1979, floods led to 1,527 dam failures, representing 51.5% of the total. Additionally, structural defects were the cause of 1,142 dam breaks, accounting for 38.5% of all dam breaks[5]. Subsequently, the number of failures caused by overtopping and quality problems decreased significantly, but the proportion remained high[6,7]. From 2001 to 2021, overtopping was responsible for 44.4% of dam failures, while quality issues accounted for 34.4%[4,8].

The leading cause of reservoir overtopping and subsequent dam break is the overflow flood, with the problem being exacerbated by engineering quality issues. Specifically, the overflow flood issue can be attributed to inadequate flood discharge capacity and excessive flood levels. The engineering quality problem encompasses insufficient seepage stability, structural stability, flood control capacity, and seismic stability. While advancements in digital technology have contributed to a decrease in flood overtopping accidents, the engineering quality issues remains unresolved. The structural instability accounts for 78.9% of the dam quality issues, and the safety risk of reservoir dam structure (RDS) is worthy of in-depth discussion[9,10].

After the completion of the reservoir dam, various factors contribute to safety issues in the RDS, including climate conditions, corrosion, oxidation, aging, and vulnerability to damage under static and live loads for a long time[11,12]. Safety monitoring is essential to ensure the structural integrity of the RDS. Through instrument monitoring, the main structure, foundation, bank slope, related facilities, and the surrounding environment can be observed and assessed to verify design specifications, enhance construction quality, and evaluate safety measures[13,14]. It includes the evaluation of dam deformation, seepage levels, stress–strain relationships, and environmental parameters. Automatic monitoring systems can assist in providing timely alerts and assessing the operational status of the RDS. Ultimately, maintaining a secure RDS is crucial for its sustained and reliable performance. The systematic analysis and assessment of RDS safety have been longstanding priorities.

Safety risk identification is indispensable to the operation of RDS. It enables engineers and managers to assess the actual condition of the RDS and promptly implement necessary repairs[15,16]. Identifying potential safety hazards and risk factors facilitates the formulation of adequate safety measures and emergency plans. The safety risk factors affecting RDS encompass three aspects: structural engineering risks, environmental risks, and personnel risks. Prominent issues include defects in dam construction quality and inadequate flood control standards[17,18]. Environmental risk factors include exceeding floods and temperature fluctuations[19]. In hydraulic projects, outdated management systems and insufficient non-engineering measures contribute to dam deterioration.

[1]School of Civil Engineering, Fuzhou University, Fuzhou 350116, China. [2]School of Civil Engineering, Central South University, Changsha 410083, China. [3]School of Civil Engineering, Changsha University, Changsha 410000, China. ✉email: 224801059@csu.edu.cn; Z20220903@ccsu.edu.cn

The initial methods of RDS were restricted to empirical and qualitative assessment, making it challenging to conduct scientifically rigorous safety risk assessments and effective safety management. With the rapid advancements in information and monitoring technology, more sophisticated theories and techniques have been employed for dam safety risk analysis. Papadrakakis et al. (2008) proposed a neural network combined with nonlinear finite element analysis for assessing the reliability of large concrete dams[20]. Anna et al. (2018) investigated the causes of dam accidents in 2018 and identified risk factors for various types of dam using Bayesian stratification models[21].

In conclusion, research on dam safety risk assessment has yielded significant results, yet there is a need for a similar assessment focusing on RDS. Enhancing the evaluation index system and criteria for RDS, establishing a standardized evaluation framework, and considering multiple indexes comprehensively are essential for meeting the requirements of safety risk assessment. Traditional evaluation methods rely heavily on static historical data, hindering real-time dynamic monitoring and evaluation capabilities. Combining real-time detection data with historical information and implementing a multi-source information fusion approach is crucial for enhancing the accuracy of evaluation outcomes[22].

The cloud model, introduced by Chinese academician Deyi Li[23], is a mathematical model that offers the advantage of processing both quantitative and qualitative data. This capability effectively enhances the accuracy and reliability of data analysis and has found widespread applications in information processing, decision analysis, and intelligent control. Previous research methods in RDS safety risk assessment have ignored the uncertainty inherent in the assessment process, but incorporating the cloud model can effectively address this issue. The model's reasoning approach incorporates soft reasoning abilities related to natural language concepts, allowing for a more comprehensive treatment of the evaluation process. Therefore, the cloud model holds promise for enhancing safety risk assessment in RDS and facilitating uncertainty analysis.

The primary advantage of the Dempster-Shafer (D-S) theory is its ability to manage uncertain information by consolidating data from various sources. Its fundamental characteristic lies in addressing uncertainty through the concepts of "evidence" and "combination." Chung-kung Lo et al. (2014) applied the D-S evidence theory to mitigate the uncertainty of seismic probability in nuclear power plants, thereby reducing the impact of randomness and cognitive biases in the entire assessment process[24]. Palash (2015) proposed that in cases of environmental technical challenges or special circumstances where actual data is insufficient to quantify the model, the possibility sampling technique can be utilized to combine the D-S framework with generalized/normal fuzzy focal elements for risk assessment of human health[25]. Thakur et al. (2018) utilized the fuzzy Delphi method to identify key factors,and incorporated the D-S theory to grade factors with lower correlation coefficients, thereby addressing the uncertainty of information fusion between factors to obtain an optimized model[26]. Sen et al. (2021) proposed a framework for assessing the disaster resilience of housing infrastructure based on the D-S theory, employing a combined approach of the Best–Worst Method and Hierarchical Evidential Reasoning[27]. The D-S evidence theory can be leveraged to manage information from various sources and types, such as expert knowledge and sensor data, by combining evidence from multiple sources to assess the safety risks of RDS. Moreover, in scenarios where sufficient observational data is lacking, the D-S evidence theory can leverage prior knowledge to improve the accuracy of analytical results. Consequently, in this study, the D-S evidence theory is applied to analyze the safety risks of RDS.

To make up for the above research gaps, this study identifies determinants of RDS and develops a framework for safety risk assessment, which is underpinned by expert consultations and empirical investigation. The research objective is to tackle the dynamic safety risk assessment in RDS and multi-source information. To this end, this study adopts a cloud model to realize the Basic probability assignment (BPA) with D-S evidence theory, incorporating weight coefficients to enhance this process. The robustness of the proposed approach is confirmed through an analysis of monitoring data.

The structure of this study is organized as follows. We discuss the related literature review in section "Methodology". Section "Results" interprets the research methodologies. In section "Discussions and conclusions", this study carried out the safety risk assessment of RDS and Empirical verification. Finally, Sect. 6 discusses and concludes this study.

Methodology

Evaluation index system

This study establishes a four-layer safety risk evaluation index system for RDS. The first layer is the target layer, which represents the safety risk evaluation result of the RDS. The second layer is the criterion layer, encompasses the categorization of monitoring projects into broader classifications to aggregate similar types of monitoring projects. The third layer is the index layer, quantifies the basic evaluation indicators of monitoring physical quantities via the prism of specific dam monitoring projects. The fourth layer is the monitoring points, is predominantly situated across various locations within and around the dam. These points collect data from monitoring devices, which serve as the foundational evaluation quantity, thereby yielding more realistic and accurate safety risk assessment results for the RDS.

Criterion layer

The safety risk assessment of RDS within the *Guidelines on Dam Safety Evaluation* is deeply analyzed[28]. This study defines the criterion layer of the evaluation index system, which includes dam deformation, dam seepage, stress–strain, and environmental quantity. Continuous monitoring of dam deformation, dam seepage, and stress and strain via sensors installed across the RDS enables real-time data capture, which offers immediate insights into the structure's safety status. In contrast, environmental are not directly monitored in this manner.

By establishing interrelationships among these parameters, the study simulates the trend of effect size over a time series, thus providing an objective reflection of the RDS.

(1) Dam deformation. Deformation issues such as cracking and tilting can arise during dam operation, significantly impacting the safety and stability of hydraulic structures. Monitoring deformation at specific locations on the dam is essential. Deformation is the primary focus of RDS system.
(2) Dam seepage. Dam seepage refers to the flow of water inside or around the dam through the dam body, resulting in water pressure and affecting the stability of the dam. The seepage state of the dam directly is a direct reflection of changes in seepage flow, making it crucial to monitor the seepage flow within the dam body, the dam foundation, and the surrounding area. The accuracy and timeliness of monitoring data are essential for ensuring the seepage safety of dams.
(3) Stress–strain. By monitoring the stress–strain behavior of the dam, it is possible to gain insight into the internal stress conditions of the dam and to promptly identify and mitigate any issues that may pose safety hazards. When the stress–strain distribution of RDS is not uniform, the stress–strain in local areas may exceed its bearing capacity, resulting in deformation, crack, and collapse. The stress–strain variation of RDS may also indirectly affect the dam seepage.
(4) Environmental quantity. Monitoring external factors can enhance the identification of potential risks and facilitate the implementation of preventive measures before these risks materialize. For example, reservoir water level monitoring can provide advance warning of potential flood overtopping and enable the analysis of whether the internal RDS can withstand the resulting flood impacts.

Index layer

This study adopts various methodologies, including field investigation, monitoring data collection, geological surveys, meteorological observation, and historical archives. Detailed information regarding the construction history, structural design, materials used, dam specifications (height and width), and spillway characteristics is gathered through meticulous observation and systematic recording. Concurrently, a thorough investigation of the surrounding environment is conducted, focusing on terrain, geomorphology, and hydrometeorological conditions. Furthermore, operational management details of the dam are scrutinized, encompassing maintenance practices and historical safety records of the RDS. Subsequently, through the analysis and synthesis of field investigation data, in conjunction with existing literature, the primary safety risk assessment indices for the RDS are established, as presented in Table 1.

Index selection

This study involved the participation of 20 experts from diverse departments and fields to ensure the scientific evaluation of indicators. The experts possess extensive experience and expertise in their respective domains. Specifically, the expert panel comprised individuals from the transport management department (two experts from the provincial Flood Prevention Office and three experts from the Hydraulic Bureau), academic professionals in

Criterion layer	Index layer	References
Dam deformation	Horizontal displacement	29
	Vertical displacement	30
	Crack width	31,32
	Dam inclination	33,34
	Slope displacement	35,36
Dam seepage	Deflection	37
	Uplift pressure	38
	Seepage flow	39,40
	Seepage around dam	41,42
	Seepage pressure	43,44
	Water quality analysis	45,46
	Groundwater table	47
Stress–strain	Stress monitoring	48
	Strain monitoring	49–51
	Dam body temperature	52,53
Environmental quantity	Reservoir level	54,55
	Environmental temperature	56
	Water temperature before dam	57
	Rainfall	58,59
	Atmospheric pressure	60
	Sedimentation in front of dam and erosion downstream	61

Table 1. Primary index.

hydraulics (two experts from Hohai University and three experts from Fuzhou University), experts in hydraulic engineering design (three senior engineers from the Fujian Hydraulic and Hydropower Survey & Design Institute and three senior engineers from the Fuzhou Hydraulic and Hydropower Planning & Design Institute), as well as experts in hydraulic engineering construction (two engineers from Fujian Hydraulic and Hydropower Engineering Bureau Co., Ltd., and two engineers from China Communications Hydraulic and Hydropower Construction Co., Ltd.).

Experts compare and rate the primary indicators to evaluate their selection, providing opinions and recommendations. Twenty expert consultation questionnaires were distributed, all of which were returned. After excluding incomplete and duplicate responses, 18 valid questionnaires were analyzed. Considering the diverse expertise among experts, average scores were computed for identical indices. Following multiple rounds of refinement, nine indicators were ultimately chosen. It is essential to note that assessing safety risks in RDS is complex. The evaluation system for actual projects should reflect RDS-specific factors such as variations in monitoring equipment placement and health conditions. The index system for evaluating RDS is categorized into four layers, illustrated in Fig. 1.

Evaluation index grade standard

The safety risk evaluation result of the RDS is divided into 5 levels, as follow:

$$\begin{aligned} V &= \{V_1, V_2, V_3, V_4, V_5\} \\ &= \{Normal, Basically\ normal, Mild\ abnormal, Severely\ abnormal, Malignant\ disorder\} \end{aligned}$$

The establishment of grading standards for evaluation indicators typically involves two primary methods: subjective and objective. Subjective judgment relies on expert experience and historical data to qualitatively assess dam safety levels, whereas objective judgment utilizes statistical data and mathematical methods to quantitatively evaluate dam safety risks. These two approaches complement each other, enabling a more accurate and comprehensive assessment. Thus, the grading criteria for evaluation indicators in this study were formulated by referencing pertinent standards, consulting expert opinions, incorporating existing scholarly research findings, and considering actual engineering conditions.

The assessment of dam deformation includes three key indexes: horizontal displacement, vertical displacement, and crack width. Horizontal and vertical displacements are two-dimensional measures, whereas crack width is unidimensional. It is important to recognize that cracks, by their nature, may exhibit closure, resulting in negative values in the data. The evaluation criteria for dam seepage encompass uplift pressure, seepage flow, and seepage around the dam. Uplift pressure is evaluated using a curtailment coefficient, while seepage flow is classified according to the volume of leakage per second. Seepage around the dam is graded using the concept of standard deviation S, according to historical data, and the five evaluation grades correspond to $[y_{\min}, \bar{y})$, $(\bar{y} + \bar{y} + s)$, $(\bar{y} + s, \bar{y} + 2s)$, $(\bar{y} + 2s, \bar{y} + 3s)$, $(\bar{y} + 3s, y_{\max}]$, $y_{\max}$ and $y_{\min}$ are the maximum and minimum values of the historical data, $\bar{y}$ and S are the mean value and standard deviation. According to the *Design Specification for Stone Masonry Dam*[62] and *Design Specification for Concrete Arch Dams*[63] issued by the

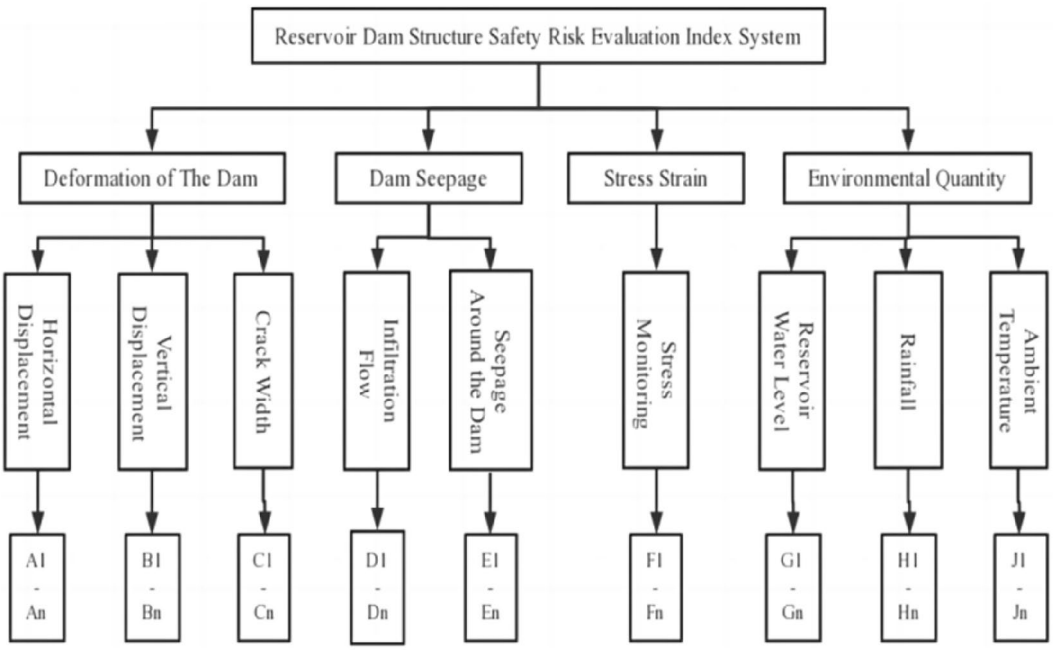

Fig. 1. Safety risk evaluation index system of RDS.

Ministry of Water Resources of the People's Republic of China, the design values for compressive stress and tensile stress of masonry arch dams are -4.1 MPa and 1.5 MPa respectively. Using the aforementioned design values as a reference point, the critical values for five evaluation levels are determined at 60%, 80%, 90%, and 100% of the baseline value for both compressive and tensile stresses. The evaluation indexes for environmental factors consist of reservoir level, rainfall, and environmental temperature. There is a general agreement among researchers regarding the assessment of these three indicators.

Evaluation model

Cloud model

The study leverages the cloud model to address the imprecision and uncertainty inherent in standard methods of evaluating index classifications, particularly when it comes to grade intervals. According to the evaluation index grade standard (Table 2), the upper and lower limits of each risk grade interval are marked as $\left[\mathrm{Xij(L)}, \mathrm{Xij(R)}\right], \mathrm{Xij(L)} > \mathrm{Xij(R)}, \mathrm{Xij(L)} \geq 0$. The calculation of the standard cloud model of grade interval is shown in Eq. (1). Each evaluation index value of the research object needs to be transformed by the membership function to become the data required by the calculation model. According to Eq. (2), the measured time series of each evaluation index and the eigenvalue of the standard cloud model are used to calculate the membership μ_{ij} of the eigenvalue of i in the j.

$$\begin{cases} Ex_{ij} = \frac{x_{ij}(L)+x_{ij}(R)}{2} \\ En_{ij} = \frac{x_{ij}(L)-x_{ij}(R)}{2.33} \\ He_{ij} = s \end{cases} \quad (1)$$

$$\mu_{ij}(p) = \exp\left(-\frac{(x_p - E_{xij})^2}{2(E_{nij'})^2}\right)$$

$$\mu_{ij} = \sum_{k=1}^{N} \frac{\mu_{ij}(p)}{N} \quad (2)$$

Ex_{ij} is the expected value of the standard cloud in the j interval of the i evaluation factor. En_{ij} is entropy. He_{ij} is super entropy. s is a constant, estimated and determined by experts according to the actual situation, and is used to express the uncertainty existing in the identification of evaluation factor interval. s ranges from 0 to Ex_{ij}. E_n' is the expectation of E_n. He is a typical random number with standard deviation. x_p is the p measured value of the time series.

Basic probability assignment matrix transformation

The membership degree of evaluation index $c_i(i = 1, 2, \ldots, n)$ belonging to safety evaluation grade $V_i(i = 1, 2, \ldots, q)$ satisfies the definition and nature of BPA. However, the membership degree sum of each evaluation grade is not 1. This study supplements the definition according to formula (3) to meet the BPA application requirements.

Category	Evaluation index	Normal	Basically normal	Mild abnormal	Severely abnormal	Malignant disorder
Dam deformation	Horizontal displacement (mm) [64–66]	[0, 20)	[20, 60)	[60, 100)	[100, 140)	[140, 200)
	Vertical displacement (mm) [64–66]	[0, 10)	[10, 30)	[30, 80)	[80, 130)	[130,, 200)
	Crack width (mm) [64–66]	[− 1.0, 0.4)	[0.4, 1.0)	[1.0, 1.6)	[1.6, 4.0)	[4.0, 10.0)
Dam seepage	Uplift pressure [64–66]	[0, 0.2)	[0.2, 0.4)	[0.4, 0.6)	[0.6, 0.8)	[0.8, 1.0)
	Seepage flow (L/s) [64–66]	[0, 2)	[2, 10)	[10, 20)	[20, 40)	[40, 80)
	Seepage around dam (m)	$[y_{min}, \bar{y})$	$[\bar{y}, \bar{y}+S)$	$[\bar{y}+S, \bar{y}+2S)$	$[\bar{y}+2S, \bar{y}+3S)$	$[\bar{y}+3S, y_{max})$
Stress–strain	Compressive stress (Mpa) [62,63,67]	[− 2.5, 0)	[− 3.3, − 2.5)	[− 3.7, − 3.3)	[− 4.1, − 3.7)	[− 10, − 4.1)
	Pull stress (Mpa) [62,63,67]	[0, 0.9)	[0.9, 1.2)	[1.2, 1.35)	[1.35, 1.5)	[1.5, 6)
Environmental quantity	Reservoir level (m) [64–66]	[− 40, − 10)	[− 10, 2)	[2, 4)	[4, 6)	[6, 8)
	Rainfall (mm/h) [64–66]	[0, 2)	[2, 4)	[4, 8)	[8, 20)	[20, 50)
	Environmental temperature (℃) [64–66]	[0, 5)	[5, 10)	[10, 20)	[20, 30)	[30, 50)

Table 2. Grade standard for safety risk evaluation index of RDS.

$$\begin{cases} \theta_i = 1 - \max(\mu_{i1}, \mu_{i1}, \ldots, \mu_{i1}) \\ m_i(X) = \theta_i \\ m_i(A_j) = \frac{(1-\theta_i)\mu_{ij}}{\sum_{j=1}^{q} \mu_{ij}} \end{cases} \tag{3}$$

$m_i(X)$ represents the probability that the decision result of the evaluation index is uncertain, which can be used as a confidence index to measure the reliability of the evaluation result. The larger the value, the higher the uncertainty of the evaluation results.

Evidence fusion and decision making

In this study, subjective and objective fusion weights are used as the weight distribution of evidence, as demonstrated in formula (4). Experts evaluate the impact of each evaluation index on the decision outcome, establishing the subjective weight, and determining the objective weight based on data characteristics.

$$\begin{cases} m(A) = m_1 \oplus m_2(A) = \begin{cases} \frac{1}{1-K} \sum\limits_{A_i \cap A_j = A} [W_1 m_1(A_i)]\left[W_2 m_2\left(A_j\right)\right], \forall A \subseteq \Theta,\ A \neq \varphi \\ 0, \qquad A = \varphi \end{cases} \\ K(m_1, m_2) = \sum\limits_{A_i \cap A_j = \varphi} [W_1 m_1(A_i)]\left[W_2 m_2\left(A_j\right)\right] < 1 \end{cases} \tag{4}$$

W_1, W_2 are the subjective and objective weights after the fusion of corresponding indicators. K is the conflict coefficient reflecting the degree of conflict between evidences. $1/(1-K)$ is the normalization coefficient used to avoid the probability of assigning non-zero to the empty set φ in the combination. The safety risk assessment results of RDS were obtained after layer fusion of each evaluation index,$m(A) = [m(A_1), m(A_2), m(A_3), m(A_4), m(A_5), m(\Theta)]$. $m(A_i)$ is the evaluation grade:

$$\{\text{Normal},\ \text{Basically normal},\ \text{Mildly abnormal},\ \text{Severely abnormal},\ \text{Malignant disorders}\}$$

According to the principle of the maximum attribute, the safety grade is selected with the maximum BPA. This study introduced the confidence index $d = 1 - m(\Theta)$ to measure the reliability of the safety risk perception results. The greater the value of the confidence index, the more reliable the fusion result of the evaluation index.

Research scenario

XY Reservoir is located in Xiyuanxi Canyon, Fuzhou City, China, serving primarily for flood control, water supply, and power generation. The reservoir spans approximately 83 km^2 with an average annual runoff of 0.9872 million m^3. It features a parabolic hyperbolic masonry arch dam, reaching a maximum dam height of 68.8 m and a crest length of 237.4 m. The total storage capacity of 24.28 million m^3, including a flood control storage capacity of 13.23 million m^3 for the main flood season, maintaining an average water level of 97.0 m. The reservoir includes a 3 MW power station and a water supply system capable of delivering 70,000 tonnes per day to the surrounding area.

XY reservoir employs a "spillway + dam top spillway" combination mode, effectively mitigating floods by delaying and reducing peak flows, thus minimizing downstream impacts during mountain flood events. In 2014, the comprehensive safety assessment of the reservoir classified it as a Class II dam. The spillway tunnel underwent reinforcement in 2016 to address cavitation and leakage issues, ensuring stable operation, high project quality, and structural safety. Additionally, the reservoir is equipped with comprehensive monitoring systems, covering dam deformation, seepage, stress–strain, and environmental parameters. An intelligent dam safety monitoring system automatically collects, processes, and provides real-time early warnings based on monitoring data, as illustrated in Fig. 2.

Fig. 2. Layout distribution map of dam monitoring points of XY Reservoir. (Author drawing).

(1) Dam deformation monitoring

In order to monitor the displacement of the dam top, foundation, and body, two GNSS monitoring points (G3 and G6) were set up at the dam base, while two additional GNSS monitoring points (G4 and G5) were set up on the surface of the dam body. Additionally, seven measuring robot-automatic total station displacement monitoring points (TR3-TR9) were set up on the dam top. Both horizontal and vertical displacements are recorded and analyzed at each monitoring point. Furthermore, seven vibrating wire remote sensing joint gauges (CF1-CF7) were installed in proximity to the dam abutment and spillway pier for the purpose of crack monitoring. It is important to mention that G1, G2, TR1, and TR2 serve as base calibration points and are not utilized for actual evaluation; therefore, they have been excluded from the analysis process.

(2) Dam seepage monitoring

Four positive displacement flowmeter seepage monitoring points (WE1-WE4) are installed on the dam abutment, complemented by five remote sensing seepage monitoring points (Z1-Z5) positioned along the left bank of the dam.

(3) Stress–strain monitoring

Four vibrating wire remote sensing strain gauges (s2-1X, s2-1Y, s2-2X, s2-2Y) have been positioned at the crest of the dam and the abutments on both the left and right sides to observe variations in stress and strain within the structure.

(4) Environmental quantity monitoring

The monitoring of water levels and temperature is conducted at various locations within the reservoir, while rainfall is monitored in multiple locations throughout the corresponding river basin.

Results

Evaluation index system

According to the actual layout of specific monitoring projects of XY reservoir dam, combined with the safety risk evaluation index system of RDS, an empirical evaluation index system has been developed, as illustrated in Fig. 3. Notably, the lifting pressure was omitted from this system, as it was not a factor addressed within the project scope.

Cloud model computing

The forward cloud generator was used to calculate the basic parameters of the cloud model *Ex*, *En*, *He*, and the safety grade interval of the XY reservoir dam structure was calculated, respectively. Moreover, MATLAB was used to generate a cloud model and draw each evaluation index's corresponding normal cloud map, as shown in Fig. 4.

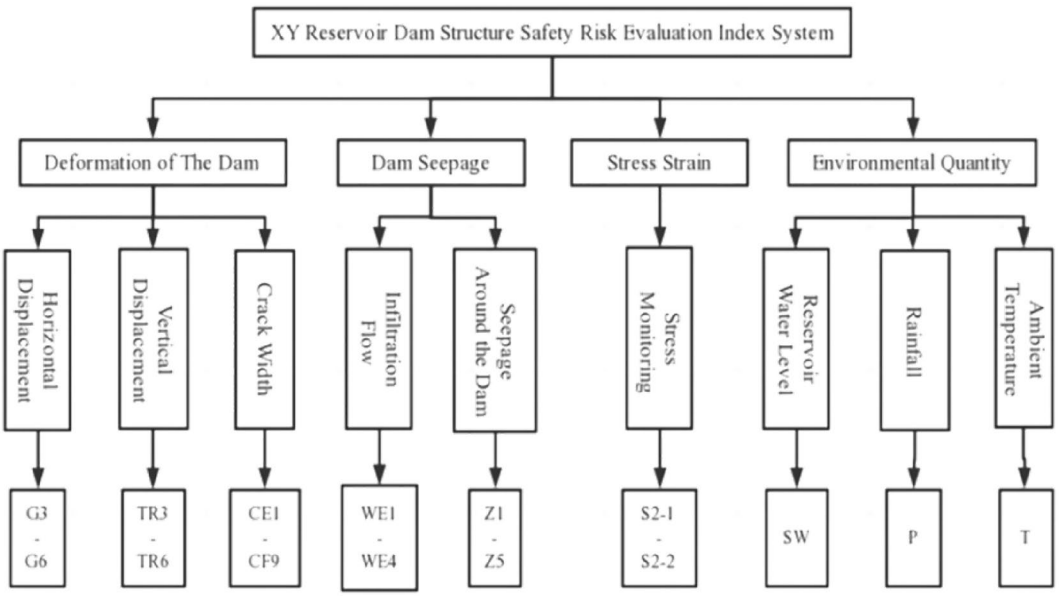

Fig. 3. XY Reservoir Dam Structure Safety Risk Evaluation Index System.

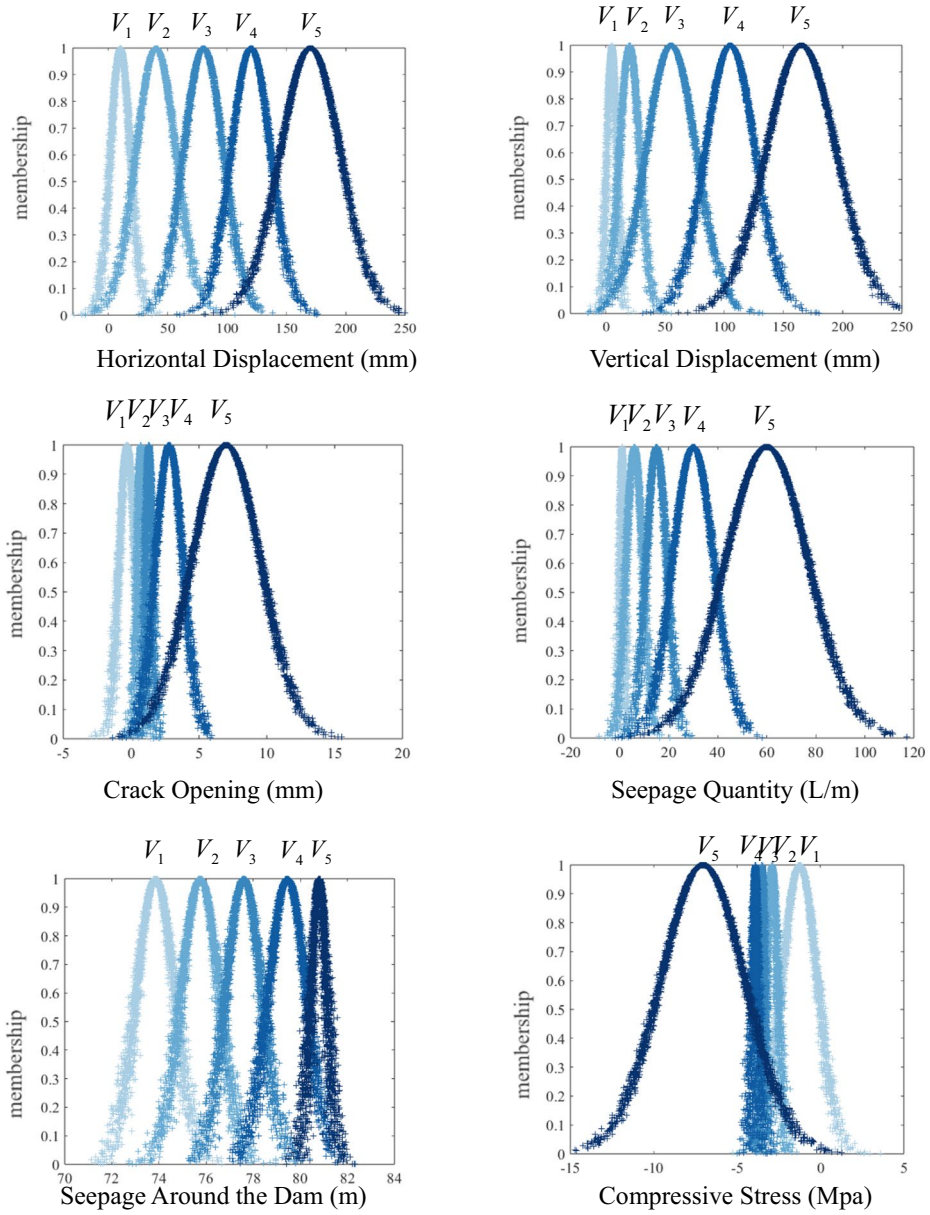

Fig. 4. Safety risk assessment level cloud map.

About 700 historical data were selected for each monitoring point and substituted into the cloud model. This process translated the data into the membership degree of the monitoring point for each corresponding monitoring index, calculating the membership grade of each location. These membership grades were then transformed into BPA scores for individual monitoring points, which are detailed Appendix.

Weight calculation

In this study, we invited 10 experts from the previously mentioned expert panel to assess the relative importance of evaluation indicators and monitoring points using the Analytic Hierarchy Process (AHP) method for. Their background information is provided in Table 3.

In the context of distinct monitoring sites encompassed within a singular project, the entropy weight approach is employed to establish the weights associated with the fusion components at each site. Conversely, for disparate monitoring endeavors, the methodology predicated on the distance function is utilized to assign weights among diverse evidence sources. This procedure facilitates the rebalancing of the BPA allocation from the evidence sources, enhancing the capacity to reflect the distinct data attributes of the various monitoring sites within the project. Consequently, the approach yields more accurate evaluations that mitigate conflicts among evidence sources, leading to fusion outcomes that are superior in terms of completeness, precision, and relevance. Subsequently, a unified weighting scheme, merging subjective and objective components, is derived through linear combination, as presented in Table 4.

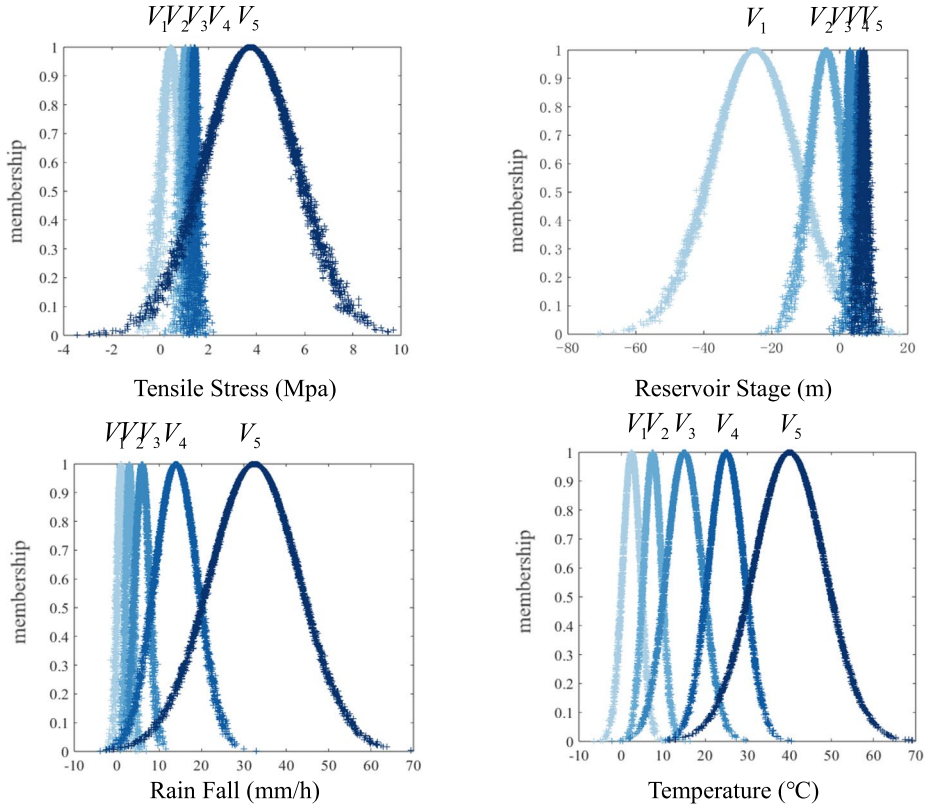

Fig. 4. (continued)

Experts	Organization	Position	Education background	Experience (years)
1	Fujian flood control office	Director	Ph.D in hydraulic engineering	24
2	Hohai University	Professor	Ph.D in hydraulic engineering	16
3	Fuzhou University	Professor	Ph.D in hydraulic engineering	15
4	Fujian Water resources and hydropower survey and design Institute	Senior engineer	Ph.D in civil engineering	10
5	Fujian Water resources and hydropower survey and design Institute	Senior engineer	Ph.D in engineering management	13
6	Fuzhou water conservancy and hydropower planning and design Institute	Senior engineer	Master in civil engineering	12
7	Fuzhou water conservancy and hydropower planning and design Institute	Senior engineer	Master in hydraulic engineering	12
8	Fujian Water Conservancy and Hydropower Engineering Bureau Co., LTD	Senior engineer	Master in hydraulic engineering	13
9	Fujian Water Conservancy and Hydropower Engineering Bureau Co., LTD	Senior engineer	Ph.D in hydraulic engineering	14
10	Zhongjiao Water Conservancy and hydropower construction Co., LTD	Senior engineer	Master in hydraulic engineering	17

Table 3. Background information of experts involved in determining the weights.

Evidence synthesis and decision making

(1) Evidence correction

Conflicting evidence must be identified and rectified prior to evidence fusion. For instance, when assessing the evaluation index through crack width, the similarity matrix for crack monitoring points is determined based on the BPA for each point. The results of this computation are presented in Table 5.

Crack width	Weight	Horizontal displacement	Weight	Vertical displacement	Weight
CF1	0.0984	G3	0.0840	G3	0.0821
CF2	0.1047	G4	0.0939	G4	0.0993
CF3	0.0677	G5	0.0920	G5	0.0952
CF4	0.0947	G6	0.0878	G6	0.0899
CF5	0.1154	TR3	0.0811	TR3	0.0836
CF6	0.1189	TR4	0.0952	TR4	0.1022
CF7	0.1357	TR5	0.0954	TR5	0.0925
CF8	0.1309	TR6	0.0900	TR6	0.0919
CF9	0.1340	TR7	0.0915	TR7	0.0881
		TR8	0.0997	TR8	0.0842
		TR9	0.0896	TR9	0.0912
Seepage flow	**Weight**	**Seepage around dam**	**Weight**	**Stress–strain**	**Weight**
WE1	0.2611	Z1	0.2148	s2−1x	0.2501
WE2	0.2173	Z2	0.2162	s2−1y	0.2486
WE3	0.2824	Z3	0.1726	s2−2x	0.2592
WE4	0.2394	Z4	0.2221	s2−2y	0.2422
		Z5	0.1745		

Table 4. Subjective and objective fusion weights.

Monitoring point	CF1	CF2	CF3	CF4	CF5	CF6	CF7	CF8	CF9
CF1	1.0000	0.2275	0.8368	0.6656	0.8937	0.7383	0.5703	0.9452	0.8833
CF2	0.2275	1.0000	0.4472	0.8426	0.1955	0.3637	0.0718	0.5081	0.2328
CF3	0.8368	0.4472	1.0000	0.8500	0.5369	0.9640	0.8395	0.8114	0.5301
CF4	0.6656	0.8426	0.8500	1.0000	0.4869	0.7800	0.5222	0.8142	0.5066
CF5	0.8937	0.1955	0.5369	0.4869	1.0000	0.3712	0.1440	0.8983	0.9972
CF6	0.7383	0.3637	0.9640	0.7800	0.3712	1.0000	0.9355	0.6800	0.3597
CF7	0.5703	0.0718	0.8395	0.5222	0.1440	0.9355	1.0000	0.4207	0.1195
CF8	0.9452	0.5081	0.8114	0.8142	0.8983	0.6800	0.4207	1.0000	0.9017
CF9	0.8833	0.2328	0.5301	0.5066	0.9972	0.3597	0.1195	0.9017	1.0000
Mean similarity	0.7512	0.4321	0.7573	0.7187	0.6137	0.6880	0.5137	0.7755	0.6145

Table 5. Similarity of monitoring points of reservoir dam crack deformation.

According to the m_i and m_j obtained from the monitoring data obtained from different monitoring points or different monitoring items, the cosine similarity is used to calculate the similarity between them. The formula is shown in Eq. (5)

$$sim(i,j) = \cos(\vec{m}_i, \vec{m}_j) = \frac{\vec{m}_i \cdot \vec{m}_j}{\|\vec{m}_i\| \cdot \left\|\vec{m}_j\right\|} \tag{5}$$

where $sim\left(i,j\right)\left(i = 1,2,,\cdots n; j = 1,2,\cdots,n\right)$ represents the similarity between the monitoring point or monitoring item and the monitoring point or monitoring item.

In order to calculate the correlation between monitoring points, the similarity matrix of monitoring points or monitoring items of the same group is constructed as follows:

$$sim = \begin{bmatrix} sim(1,1) & \cdots & sim\left(1,j\right) & \cdots & sim(1,n) \\ \cdots & & \cdots & & \cdots \\ sim(i,1) & \cdots & sim\left(i,j\right) & \cdots & sim(i,n) \\ \cdots & & \cdots & & \cdots \\ sim(n,1) & \cdots & sim\left(n,j\right) & \cdots & sim(n,n) \end{bmatrix} \tag{6}$$

For each row of the matrix, the values are aggregated to obtain the total similarity of each monitoring point relative to all other monitoring points, and the total similarity is averaged to obtain the mean similarity, denoted as $sim(i)$:

$$sim(i) = \frac{\sum_{j=1}^{n} sim(i,j)}{n} \tag{7}$$

The similarity of the monitoring point or item i compared with other monitoring points or items can be clearly seen through the mean similarity $sim(i)$. A large similarity indicates that there is no evidence conflict between the evidence of the monitoring point or item and that of other monitoring points or items. Conversely, the low similarity indicates evidence conflict between the evidence from one monitoring site or item and evidence from other monitoring sites or items.

By integrating academic research with practical application, this study establishes a similarity threshold of 0.7. Evidence with a similarity score above this threshold is considered to be in substantial agreement with other evidence, thus it can be directly employed in calculations. Conversely, when the similarity score falls below 0.7, substantial inconsistency exists between the evidence in question and other evidence, necessitating modification of the source to mitigate these conflicts before its use in calculations. This approach not only resolves the paradoxes stemming from conflicting evidence in fusion outcomes but also safeguards the integrity and efficacy of the fusion results. According to the mean similarity, the mean similarity of CF2, CF5, CF6, CF7, and CF9 is lower than 0.7, which requires evidence correction. According to the crack width of the weighted objective weight and evidence, a weighted average of evidence. $\bar{m}$ = (0.2740,0.2353,0.0178,0.0490,0.0197,0.4043). Utilizing the weighted mean approach, discrepant evidence is reconciled to derive a revised primary probability distribution, as depicted in Table 6. The correction of evidence has mitigated the discrepancies in probabilities among the evidence sets, thereby lessening the conflicts among them.

(2) Evidence synthesis

The new fracture deformation fusion result is obtained after the evidence replacement, according to the improved evidence synthesis fusion formula. Subsequently, these results were compared with those calculated by the traditional D-S evidence theory algorithm, as shown in Table 7.

Compared with the results, the improved algorithm based on the D-S evidence theory has outstanding advantages over the traditional algorithm. On the one hand, the BPA by the traditional algorithm for the standard and regular evaluation grade is 0.5556 and 0.4260, and the difference between the values is close and not obvious. The BPA of the improved algorithm's regular and average evaluation grades are 0.6250 and 0.3565; the difference is noticeable, and the uncertainty of the decision is better reduced. On the other hand, the comparison shows that the confidence degree $d = 1 - m(\Theta)$ increases from 0.9893 to 0.9964, which reflects that the fusion result obtained by the improved algorithm holds better reliability.

According to the improved D-S evidence fusion algorithm, weight is added to the fusion process. The evidence fusion is executed at each monitoring point, resulting in the determination of probability distribution functions for each evaluative index. Subsequently, dynamic weights are computed, and these are amalgamated with subjective weights to yield an integrated measure of subjective and objective fusion weights. This composite weight is further refined through an additional fusion process, culminating in the allocation of BPA for comprehensive evaluation, as shown in Table 8.

Monitoring point	m_1	m_2	m_3	m_4	m_5	m_X
CF1	0.3061	0.0864	0.0236	0.0351	0.0205	0.5283
CF2	0.2740	0.2353	0.0178	0.0490	0.0197	0.4043
CF3	0.4045	0.1989	0.0675	0.0813	0.0166	0.2312
CF4	0.2457	0.4416	0.0297	0.0573	0.0168	0.2088
CF5	0.2740	0.2353	0.0178	0.0490	0.0197	0.4043
CF6	0.2740	0.2353	0.0178	0.0490	0.0197	0.4043
CF7	0.2740	0.2353	0.0178	0.0490	0.0197	0.4043
CF8	0.1906	0.2441	0.0073	0.0571	0.0149	0.4860
CF9	0.2740	0.2353	0.0178	0.0490	0.0197	0.4043

Table 6. BPA distribution after modification of reservoir dam crack deformation monitoring site.

Evaluation index	m_1	m_2	m_3	m_4	m_5	m_X
Improved DS algorithm	0.6250	0.3565	0.0034	0.0095	0.0021	0.0036
Traditional DS algorithm	0.5556	0.4260	0.0006	0.0058	0.0013	0.0107

Table 7. Fusion results of the improved algorithm and traditional algorithm.

Evaluation index	m_1	m_2	m_3	m_4	m_5	m_X
Structural safety	0.9902	0.0052	0	0	0.0034	0.0012

Table 8. BPA distribution in the overall safety risks of RDS.

(3) Evaluation decision

According to the principle of the maximum attribute, the maximum value of $m(A_i)$ is 0.9902, which corresponds to the evaluation grade of "normal," and the safety grade of the dam structure of the reservoir is judged to be safe. The evaluation results are consistent with the expert's evaluation of the safety state of the dam operation. It also verifies the feasibility and rationality of the evaluation model proposed in this study. According to the confidence index $d = 1 - m(\Theta) = 0.9988$, the reliability of this evaluation result is high and proves the feasibility and rationality of the safety risk assessment model of RDS proposed.

Evaluation of measured data

In practical engineering, it is necessary to evaluate RDS by historical monitoring data and evaluate the real-time safety state. In this study, we employed measured data to substitute into an evaluation model constructed from historical data for fusion. Specifically, monitoring data on March 19, 2023, were selected, as shown in Table 9. The measured data were incorporated into the fusion method using the identical steps previously described. Subsequently, through layer-upon-layer fusion, the real-time safety risk assessment results of RDS under the background of the measured data were finally obtained, as shown in Table 10.

Discussions and conclusions

In this study, we developed a safety risk evaluation index system of RDS that primarily focuses on monitoring data. The system integrates industry norms, field research, relevant literature, and expert interviews. The index system can predict and identify the RDS, allowing for appropriate preventive and responsive actions to mitigate potential losses. Additionally, it fosters the advancement of hydraulic industry standardization and enhances management practices.

Secondly, aiming at the uncertainty and fuzziness in the safety risk analysis of RDS, the cloud model is introduced to blur the evaluation level. The cloud model ascertains the BPA for each index of evidence through the membership degrees derived from the evidence theory. This approach rectifies the limitations of evidence

Crack width	Value	Horizontal displacement X	Value	Horizontal displacement Y	Value	Vertical displacement	Value
CF1	0.425	G3	− 0.155	G3	1.755	G3	8.526
CF2	− 0.449	G4	− 0.865	G4	10.652	G4	0.562
CF3	0.426	G5	2.322	G5	15.233	G5	5.992
CF4	0.565	G6	1.525	G6	1.322	G6	3.233
CF5	0.095	TR3	− 1.056	TR3	− 0.865	TR3	− 2.25
CF6	− 0.322	TR4	− 0.484	TR4	1.365	TR4	1.252
CF7	0.326	TR5	− 0.793	TR5	− 0.006	TR5	− 0.855
CF8	0.366	TR6	− 0.855	TR6	12.04	TR6	3.235
CF9	− 0.326	TR7	2.955	TR7	17.45	TR7	0.523
		TR8	− 0.474	TR8	− 1.235	TR8	− 1.655
		TR9	− 0.366	TR9	1.365	TR9	1.545
Seepage flow	**Value**	**Seepage around dam**	**Value**	**Stress–strain**	**Value**	**Others**	**Value**
WE1	0	Z1	89.265	s2−1x	− 0.1570	SW	88.014
WE2	0	Z2	76.523	s2−1y	0.1317	P	0
WE3	0	Z3	72.023	s2−2x	− 0.0583	T	13.6
WE4	0.007	Z4	76.665	s2−2y	− 0.3223		
		Z5	74.325				

Table 9. Monitoring data value summary.

Evaluation index	m_1	m_2	m_3	m_4	m_5	m_X
Structural safety	0.9212	0.0429	0.0016	0.0009	0.0025	0.0309

Table 10. Real-time BPA distribution of overall safety risks of reservoir dams structure.

theory when handling time series data, enhancing accuracy. Consequently, this model facilitates evidence-based decisions regarding operational modes and can potentially prolong the service life of RDS.

Finally, the traditional D-S evidence theory algorithm has been enhanced to mitigate the subjectivity and uncertainty in the evaluation process. This improvement enhances the fusion efficiency and reliability of evaluation information, effectively addressing the integration of multi-source data and resolving discrepancies in conflicting evidence. Application of the refined algorithm is demonstrated through a safety risk analysis of the XY reservoir project in Fujian Province. The results align with the current conditions, thus validating the reliability and applicability of the approach. The ability to monitor and evaluate in real-time facilitates the timely identification and resolution of existing safety concerns, thereby preempting operational risks associated with structural damage.

A thorough and judicious safety risk assessment of RDS is a crucial for bolstering emergency response capabilities and enhancing early warning systems for RDS incidents. Continuous monitoring is pivotal within the risk assessment framework. The advancement of contemporary monitoring technologies is instrumental in enhancing the proficiency and precision of safety management practices. (1) The deployment of sensors and monitoring apparatuses allows for the real-time observation of RDS attributes, including displacement, water levels, and water temperatures. Automated systems aggregation and analysis of this data facilitate the early identification and forecasting of potential security threats. (2) Computer-aided numerical simulations are effective in predicting how RDS behave under diverse operational conditions, such as seepage, earthquake, and flood scenarios. Such simulations aid in the more informed evaluation and optimization of structural design for RDS. (3) By amassing extensive data sets and employing artificial intelligence algorithms, the safety condition of RDS can be predicted and potential risks warned against, enabling proactive identification and mitigation of safety concerns. (4) A virtual reality environment can be established to replicate various operational states of RDS, including extreme conditions(i.e., earthquakes and floods) to evaluate the safety performance better. (5) Utilizing wireless sensor networks can enable the real-time tracking of RDS parameters, including water levels, temperatures, and wind speeds. Furthermore, these sensors can transmit data in real-time to a central monitoring hub, ensuring the timely acquisition of the dam's condition and the prompt recognition and management of latent safety risks.

The process of establishing grading standards presents an unusually complex challenge within academic research. Owing to the constraints on research resources, the standards proposed in this study are undoubtedly imperfect and require substantial refinement in subsequent inquiries. The grading criteria for evaluation indices are not rigid, invariable thresholds but rather should be situated within a range that is informed by real-world conditions, persistent monitoring data, and insights derived from expert scholarly analysis.

Due to a paucity of data from actual engineering projects, this study relies on only one year of historical data for foundational training. While this sufficed for meeting the specific training needs, a more protracted period of historical data is essential to anchor foundational training in the realm of big data. Subsequent research could consider incorporating an extended dataset to enhance the model's reliability.

Although the evaluation model has been established in this study, it is still necessary to further improve the evaluation system and realize visualization. By visualizing the results, project decision-makers can gain a clearer understanding of the influencing factors and evaluation outcomes, allowing them to develop effective risk management strategies. Future research may investigate methods for visualizing evaluation results and integrating the evaluation system with a decision support system to enhance services in engineering practice.

Data availability

All authors are responsible for the accuracy and validity of the data and are willing to make it available for Scientific Reports.

Received: 11 January 2024; Accepted: 26 August 2024
Published online: 30 August 2024

References

1. Tian, S., Dai, X., Wang, G., Lu, Y. & Chen, J. Formation and evolution characteristics of dam breach and tailings flow from dam failure: An experimental study. *Nat. Hazards* **107**(2), 1621–1638. https://doi.org/10.1007/s11069-021-04649-1 (2021).
2. Li, M. *et al.* A new method for intelligent prediction of drilling overflow and leakage based on multi-parameter fusion. *Energies* https://doi.org/10.3390/en15165988 (2022).
3. Zhong, C., Lu, J. A. & Kang, D. Design and experimental research of a wellhead overflow monitoring system for open-circuit drilling of natural gas hydrate. *Energies* https://doi.org/10.3390/en15249606 (2022).
4. Sheng, J. B., Li, H. E. & Sheng, T. Z. Statistical analysis of dam failure and its loss of life in China. *Hydro-Sci. Eng.* **01**, 1–15 (2023).
5. Engineering Administration Bureau of the Ministry of Water Resources. (1981). National reservoir dam collapse register. Beijing: Engineering Administration Bureau of the Ministry of Water Resources
6. Engineering Administration Bureau of the Ministry of Water Resources. (1993). National reservoir dam collapse register (1981–1990). Beijing: Engineering Administration Bureau of the Ministry of Water Resources
7. Ru, N. H. & Jiang, Z. S. *Arch Dams·Accident and Safety of Large Dams* (China Water Power Press, 1995).
8. Li, H. E., Ma, G. Z., Wang, F., Rong, W. J. & He, Y. J. Analysis of dam failure trend of China from 2000 to 2018 and improvement suggestions. *Hydro-Sci. Eng.* **05**, 101–111 (2021).
9. Zhang, G., Liu, Y. & Zhou, Q. Study on real working performance and overload safety factor of high arch dam. *Sci. China Ser. E-Technol. Sci.* **51**, 48–59. https://doi.org/10.1007/s11431-008-6012-3 (2008).
10. Jin, F. *et al.* Comparative study procedure for the safety evaluation of high arch dams. *Comput. Geotech.* **38**(3), 306–317. https://doi.org/10.1016/j.compgeo.2010.10.008 (2011).
11. Wieland, M. Safety aspects of sustainable storage dams and earthquake safety of existing dams. *Engineering* **2**(3), 325–331. https://doi.org/10.1016/J.ENG.2016.03.011 (2016).
12. Toledo, M. A. & Moran, R. Dam safety-overtopping and geostructural risks. *Water* **14**(18), 63. https://doi.org/10.3390/w14182826 (2022).

13. Suwatthikul, J. *et al.* Development of dam safety remote monitoring and evaluation system. *J. Dis. Res.* **16**(4), 607–617. https://doi.org/10.20965/jdr.2021.p0607 (2021).
14. Han, Z., Li, Y., Zhao, Z. & Zhang, B. An online safety monitoring system of hydropower station based on expert system. *Energy Rep.* **8**, 1552–1567. https://doi.org/10.1016/j.egyr.2022.02.040 (2022).
15. Morales-Torres, A., Serrano-Lombillo, A., Escuder-Bueno, I. & Altarejos-Garcia, L. The suitability of risk reduction indicators to inform dam safety management. *Struct. Infrastruct. Eng.* **12**(11), 1465–1476. https://doi.org/10.1080/15732479.2015.1136830 (2016).
16. Lu, X. *et al.* Bayesian network safety risk analysis for the dam-foundation system using Monte Carlo simulation. *Appl. Soft Comput.* **5**, 126. https://doi.org/10.1016/j.asoc.2022.109229 (2022).
17. Ge, W., Li, Z., Liang, R. Y., Li, W. & Cai, Y. Methodology for establishing risk criteria for dams in developing countries, case study of China. *Water Resour. Manag.* **31**(13), 4063–4074. https://doi.org/10.1007/s11269-017-1728-0 (2017).
18. Su, H., Yan, X., Liu, H. & Wen, Z. Integrated multi-level control value and variation trend early-warning approach for deformation safety of arch dam. *Water Resour. Manag.* **31**(6), 2025–2045. https://doi.org/10.1007/s11269-017-1631-8 (2017).
19. Colomer Mendoza, F. J. & Gallardo Izquierdo, A. Environmental risk index: A tool to assess the safety of dams for leachate. *J. Hazard. Mater.* **162**(1), 1–9. https://doi.org/10.1016/j.jhazmat.2008.05.018 (2009).
20. Papadrakakis, M. *et al.* Vulnerability analysis of large concrete dams using the continuum strong discontinuity approach and neural networks. *Struct. Saf.* **30**(3), 217–235. https://doi.org/10.1016/j.strusafe.2006.11.005 (2008).
21. Kalinina, A., Spada, M. & Burgherr, P. Application of a Bayesian hierarchical modeling for risk assessment of accidents at hydropower dams. *Saf. Sci.* **110**, 164–177. https://doi.org/10.1016/j.ssci.2018.08.006 (2018).
22. Badr, A., Yosri, A., Hassini, S. & El-Dakhakhni, W. Coupled continuous-time markov chain-bayesian network model for dam failure risk prediction. *J. Infrastruct. Syst.* **27**(4), 63. https://doi.org/10.1061/(ASCE)IS.1943-555X.0000649 (2021).
23. Li, D. & Yi, Du. *Artificial Intelligence with Uncertainty* (CRC Press, 2007).
24. Lo, C. K., Pedroni, N. & Zio, E. Treating uncertainties in a nuclear seismic probabilistic risk assessment by means of the Dempster-Shafer theory of evidence. *Nucl. Eng. Technol.*. **46**(1), 11–26 (2014).
25. Dutta, P. Uncertainty modeling in risk assessment based on Dempster-Shafer theory of evidence with generalized fuzzy focal elements. *Fuzzy Inf. Eng.* **7**(1), 15–30 (2015).
26. Thakur, G. S. M., Bhattacharyya, R. & Sarkar, S. Stock portfolio selection using Dempster-Shafer evidence theory. *J. King Saud Univ.-Comput. Inf. Sci.* **30**(2), 223–235 (2018).
27. Sen, M. K., Dutta, S. & Kabir, G. Development of flood resilience framework for housing infrastructure system: Integration of best-worst method with evidence theory. *J. Clean. Prod.* **290**, 125197 (2021).
28. Ministry of Water Resources of the People's Republic of China. (2017). *Guidelines on Dam Safety Evaluation SL 258–2017*. China Water & Power Press
29. Pan, B., Quan, Z., Huang, X. & Sun, G. Using the FA-NAR dynamic neural network model and big data to monitor dam safety. *Front. Phys.* https://doi.org/10.3389/fphy.2022.859172 (2022).
30. El-Askary, H. *et al.* Assessing the vertical displacement of the grand ethiopian renaissance dam during its filling using DInSAR technology and its potential acute consequences on the downstream countries. *Rem. Sens.* https://doi.org/10.3390/rs13214287 (2021).
31. Li, X. *et al.* Analysis of crack opening in high arch dams subjected to extremely strong earthquake. *Dis. Adv.* **6**, 214–220 (2013).
32. Soysal, B. F. & Arici, Y. Crack width-seismic intensity relationships for concrete gravity dams. *J. Earthqu. Eng.* https://doi.org/10.1080/13632469.2023.2220048 (2023).
33. Horiguchi, T. & Komatsu, Y. Method to evaluate the effect of inclination angle of steel open-type check dam on debris flow impact load. *Int. J. Protect. Struct.* **10**(1), 95–115. https://doi.org/10.1177/2041419618789702 (2019).
34. Zhang, Y., Zhong, W., Li, Y. & Wen, L. A deep learning prediction model of DenseNet-LSTM for concrete gravity dam deformation based on feature selection. *Eng. Struct.* **295**, 116827. https://doi.org/10.1016/j.engstruct.2023.116827 (2023).
35. He, P. & Li, Y. A data-driven dam deformation forecasting and interpretation method using the measured prototypical temperature data. *Water* https://doi.org/10.3390/w14162538 (2022).
36. Javdanian, H., Zarei, M. & Shams, G. Estimating seismic slope displacements of embankment dams using statistical analysis and numerical modeling. *Model. Earth Syst. Environ.* **9**(1), 389–396. https://doi.org/10.1007/s40808-022-01505-4 (2023).
37. Li, Z. *et al.* Deflection statistical monitoring model identification of the concrete gravity dam based on uncertainty analysis. *Struct. Control Health Monit.* https://doi.org/10.1002/stc.3026 (2022).
38. Ma, C., Zhao, T., Li, G., Zhang, A. & Cheng, L. Intelligent anomaly identification of uplift pressure monitoring data and structural diagnosis of concrete dam. *Appl. Sci.-Basel* **12**(2), 36. https://doi.org/10.3390/app12020612 (2022).
39. Li, S.-Y., Li, Y.-L., Si, Z. & Zhang, X.-F. A seepage computational model of face slab cracks based on equi-width joint constant flow. *Adv. Eng. Softw.* **41**(7–8), 1000–1004. https://doi.org/10.1016/j.advengsoft.2010.04.004 (2010).
40. Zhou, G. G. D., Li, S., Lu, X. & Tang, H. Large-scale landslide dam breach experiments: Overtopping and "overtopping and seepage" failures. *Eng. Geol.* https://doi.org/10.1016/j.enggeo.2022.106680 (2022).
41. Chai, J. R., Wu, Y. Q. & Li, S. Y. Analysis of coupled seepage and stress fields in rock mass around the Xiaowan arch dam. *Commun. Numer. Methods Eng.* **20**(8), 607–617. https://doi.org/10.1002/cnm.699 (2004).
42. Asadollah, S. N., Aalianvari, A. & Hajialibeigi, H. Role of geological structures in seepage from Lar dam reservoir. *Arab. J. Geosci.* https://doi.org/10.1007/s12517-018-3967-7 (2018).
43. Rice, J. D. & Duncan, J. M. Deformation and cracking of seepage barriers in dams due to changes in the pore pressure regime. *J. Geotech. Geoenviron. Eng.* **136**(1), 16–25. https://doi.org/10.1061/(ASCE)GT.1943-5606.0000241 (2010).
44. Chai, J. & Cui, W. Optimum thickness of curtain grouting on dam foundation with minimum seepage pressure resultant. *Struct. Multidiscip. Optim.* **45**(2), 303–308. https://doi.org/10.1007/s00158-011-0699-7 (2012).
45. Totsuka, S., Kageyama, Y., Ishikawa, M., Kobori, B. & Nagamoto, D. Noise removal method for unmanned aerial vehicle data to estimate water quality of Miharu dam reservoir, Japan. *J. Adv. Comput. Intell. Intell. Inf.* **23**(1), 34–41. https://doi.org/10.20965/jaciii.2019.p0034 (2019).
46. Kim, J. *et al.* Evaluation of temporal contribution of groundwater to a small lake through analyses of water quantity and quality. *Water* https://doi.org/10.3390/w12102879 (2020).
47. Abd-Elhamid, H., Abdelaty, I. & Sherif, M. Evaluation of potential impact of Grand Ethiopian Renaissance Dam on Seawater Intrusion in the Nile Delta Aquifer. *Int. J. Environ. Sci. Technol.* **16**(5), 2321–2332. https://doi.org/10.1007/s13762-018-1851-3 (2019).
48. Niu, J. *et al.* A monitoring model for the stress on a super-high arch dam during pre-impoundment construction. *Water Sup.* **20**(8), 3604–3614. https://doi.org/10.2166/ws.2020.225 (2020).
49. Ren, L., Chen, J., Li, H.-N., Song, G. & Ji, X. Design and application of a fiber Bragg grating strain sensor with enhanced sensitivity in the small-scale dam model. *Smart Mater. Struct.* https://doi.org/10.1088/0964-1726/18/3/035015 (2009).
50. Yavasoglu, H. H. *et al.* Monitoring the deformation and strain analysis on the Ataturk Dam, Turkey. *Geom. Nat. Hazards Risk* **9**(1), 94–107. https://doi.org/10.1080/19475705.2017.1411400 (2018).
51. Pilz, M., Isken, M. P., Fleming, K., Orunbaev, S. & Moldobekov, B. Long- and short-term monitoring of a dam in response to seasonal changes and ground motion loading: The test case of the Kurpsai dam, Western Kyrgyz Republic. *Pure Appl. Geophys.* **178**(10), 4001–4020. https://doi.org/10.1007/s00024-021-02861-5 (2021).

52. Zhu, M., Chen, B., Gu, C., Wu, Y. & Chen, W. Optimized multi-output LSSVR displacement monitoring model for super high arch dams based on dimensionality reduction of measured dam temperature field. *Eng. Struct.* https://doi.org/10.1016/j.engstruct.2022.114686 (2022).
53. Gu, C. *et al.* Multi-output displacement health monitoring model for concrete gravity dam in severely cold region based on clustering of measured dam temperature field. *Struct. Health Monitor. Int. J.* https://doi.org/10.1177/14759217221142006 (2023).
54. Pouraminian, M., Pourbakhshian, S. & Noroozinejad Farsangi, E. Reliability assessment and sensitivity analysis of concrete gravity dams by considering uncertainty in reservoir water levels and dam body materials. *Civil Environ. Eng. Rep.* **30**(1), 1–17. https://doi.org/10.2478/ceer-2020-0001 (2020).
55. Zhang, J., Min, Y., Feng, B. & Duan, W. Research and application of key technologies for dynamic control of reservoir water level in flood season. *Water* https://doi.org/10.3390/w13243576 (2021).
56. Yu, X., Li, J. & Kang, F. A hybrid model of bald eagle search and relevance vector machine for dam safety monitoring using long-term temperature. *Adv. Eng. Inf.* https://doi.org/10.1016/j.aei.2022.101863 (2023).
57. Zheng, X., Shen, Z., Wang, Z., Qiang, S. & Yuan, M. Improvement and verification of one-dimensional numerical algorithm for reservoir water temperature at the front of dams. *Appl. Sci.-Basel* https://doi.org/10.3390/app12125870 (2022).
58. Su, Z., Chen, G. & Meng, Y. Study on seepage characteristics and stability of core dam under the combined action of the variation of reservoir water level and rainfall. *Geotech. Geol. Eng.* **39**(1), 193–211. https://doi.org/10.1007/s10706-020-01486-0 (2021).
59. Yun, S.-K., Kim, J., Im, E.-S. & Kang, G. Relationships among seepage, water level, and rainfall of a fill dam by decision tree analysis. *Geofluids* https://doi.org/10.1155/2022/9253324 (2022).
60. Guo, W., Zeng, W., Gao, X. & Ren, Y. Analysis of air-inflated rubber dam for flood-fighting at the subway entrance. *J. Flood Risk Manag.* https://doi.org/10.1111/jfr3.12872 (2023).
61. Munoz-Salinas, E., Castillo, M., Romero, F. & Correa-Metrio, A. Understanding sedimentation at the El Molinito reservoir (NW Mexico) before and after dam construction using physical sediment analyses. *J. South Am. Earth Sci.* **6**, 111. https://doi.org/10.1016/j.jsames.2021.103401 (2021).
62. Ministry of Water Resources of the People's Republic of China. (2006). *Design Specification for Stone Masonry Dam SL 25–2006*. China Water & Power Press
63. Ministry of Water Resources of the People's Republic of China. (2003). *Design Specification for Concrete Arch Dams SL 282–2003*. China Water & Power Press
64. Pei, L., Chen, C., He, K. & Lu, X. System reliability of a gravity dam-foundation system using Bayesian networks. *Reliab. Eng. Syst. Saf.* **218**, 108178 (2022).
65. Guo, Z., Su, H., Liu, B. & He, Y. Cloud model and evidence theory-based method for comprehensive assessment on dam safety. *Water Resour. Hydropower Eng.* **3**, 99–103. https://doi.org/10.13928/j.cnki.wrahe.2017.03.018 (2017).
66. He, J., Ma, C. & Shi, Y. Multi-effect-quantity fusion model of high arch dam based on improved D-S evidence theory. *Geom. Inf. Sci. Wuhan Univ.* **12**, 1397–1400. https://doi.org/10.13203/j.whugis2012.12.001 (2012).
67. Dwivedi, Y. K. *et al.* Metaverse beyond the hype: Multidisciplinary perspectives on emerging challenges, opportunities, and agenda for research, practice and policy. *Int. J. Inf. Manag.* https://doi.org/10.1016/j.ijinfomgt.2022.102542 (2022).

Acknowledgements

Our research has been reviewed and approved by the Ethics Committee of Fuzhou University. The study complies with all regulations and confirmation. Informed consent was obtained from all participants in the study. All methods were carried out in accordance with relevant guidelines and regulations. All experimental protocols were approved. Informed consent was obtained from all subjects and their legal guardian.

Author contributions

D.Y., J.W., Z.G. and X.Z. wrote the main manuscript text and Qianqian Zhang prepared figures and tables. All authors reviewed the manuscript.

Competing interests

The authors declare no competing interests.

Additional information

Supplementary Information The online version contains supplementary material available at https://doi.org/10.1038/s41598-024-71156-1.

Correspondence and requests for materials should be addressed to Z.G. or X.Z.